



Amygdalar CB2 cannabinoid receptor mediates fear extinction deficits promoted by orexin-A/hypocretin-1

Marc Ten-Blanco^a, África Flores^{b,1}, Inmaculada Pereda-Pérez^a, Fabiana Piscitelli^c, Cristina Izquierdo-Luengo^a, Luigia Cristino^c, Julián Romero^a, Cecilia J. Hillard^d, Rafael Maldonado^b, Vincenzo Di Marzo^{c,e}, Fernando Berrendero^{a,*}

^a Instituto de Investigaciones Biosanitarias, Facultad de Ciencias Experimentales, Universidad Francisco de Vitoria, Pozuelo de Alarcón, 28223 Madrid, Spain

^b Laboratory of Neuropharmacology, Department of Experimental and Health Sciences, Universitat Pompeu Fabra, PRBB, 08003 Barcelona, Spain

^c Endocannabinoid Research Group, Institute of Biomolecular Chemistry (ICB), National Research Council (CNR), Pozzuoli, Italy

^d Department of Pharmacology and Toxicology and Neuroscience Research Center, Medical College of Wisconsin, Milwaukee, WI 53226, USA

^e Canada Excellence Research Chair on the Microbiome-Endocannabinoidome Axis in Metabolic Health, Faculty of Medicine and Faculty of Agriculture and Food Sciences, Hearsh and Lung Research Institute (IUCPO), Institute of Nutrition and Functional Foods (INAF) and NUTRISS Center, Université Laval, Quebec City, Canada

ARTICLE INFO

Keywords:

Orexin
Fear extinction
Amygdala
2-AG
CB2R
Microglia

Chemical compounds studied in this article:

URB597 (PubChem CID: 1383884)
JZL184 (PubChem CID: 25021165)
Orexin-A (PubChem CID: 92131430)
O7460 (PubChem CID: 132285144)
Rimonabant (PubChem CID: 104849)
AM630 (PubChem CID: 4302963)
JWH133 (PubChem CID: 6918505)
PLX5622 (PubChem CID: 52936034)

ABSTRACT

Anxiety and stress disorders are often characterized by an inability to extinguish learned fear responses. Orexins/hypocretins are involved in the modulation of aversive memories, and dysregulation of this system may contribute to the aetiology of anxiety disorders characterized by pathological fear. The mechanisms by which orexins regulate fear are unknown. Here we investigated the role of the endogenous cannabinoid system in the impaired fear extinction induced by orexin-A (OXA) in male mice. The selective inhibitor of 2-arachidonoylglycerol (2-AG) biosynthesis O7460 abolished the fear extinction deficits induced by OXA. Accordingly, increased 2-AG levels were observed in the amygdala and hippocampus of mice treated with OXA that do not extinguish fear, suggesting that high levels of this endocannabinoid are related to poor extinction. Impairment of fear extinction induced by OXA was associated with increased expression of CB2 cannabinoid receptor (CB2R) in microglial cells of the basolateral amygdala. Consistently, the intra-amygdala infusion of the CB2R antagonist AM630 completely blocked the impaired extinction promoted by OXA. Microglial and CB2R expression depletion in the amygdala with PLX5622 chow also prevented these extinction deficits. These results show that overactivation of the orexin system leads to impaired fear extinction through 2-AG and amygdalar CB2R. This novel mechanism could be of relevance for the development of novel potential approaches to treat diseases associated with inappropriate retention of fear, such as post-traumatic stress disorder, panic anxiety and phobias.

Abbreviations: 2-AG, 2-arachidonoylglycerol; AEA, anandamide; AM630, 6-Iodo-2-methyl-1-[2-(4-morpholinyl)ethyl]-1 H-indol-3-yl(4-methoxyphenyl)methanone; ANOVA, analysis of variance; BLA, basolateral amygdala; CB1R, cannabinoid receptor-1; CB2R, cannabinoid receptor-2; CSF1R, colony stimulating factor 1 receptor; CX3CR1, C-X3-C motif chemokine receptor 1; DAGL, diacylglycerol lipase; DMSO, dimethyl sulfoxide; ECS, endocannabinoid system; eGFP, enhanced green fluorescent protein; FAAH, fatty acid amide hydrolase; GABA, γ -aminobutyric acid; Iba1, ionized-calcium binding adapter 1; JZL184, 4-[Bis(1,3-benzodioxol-5-yl)hydroxymethyl]-1-piperidinecarboxylic acid 4-nitrophenyl ester; JWH133, (6aR,10aR)-3-(1,1-Dimethylbutyl)-6a,7,10,10a-tetrahydro-6,6,9-trimethyl-6 H-dibenzo[b,d]pyran; MAGL, monoacylglycerol lipase; NAPE-PLD, N-acyl phosphatidylethanolamine phospholipase D; O7460, 2-[(fluoromethylphosphinyl)oxy]-1-[(1-methylethoxy)methyl]ethyl ester, 9Z-octadecenoic acid; OX1R, orexin receptor-1; OXA, orexin-A; PLX5622, 5-fluoro-N-[6-fluoro-5-[(5-methyl-1 H-pyrrolo[2,3-b]pyridin-3-yl)methyl]-2-pyridinyl]-2-methoxy-3-pyridinethanamine; PTSD, post-traumatic stress disorder; URB597, cyclohexylcarbamic acid 3'-(Amino-carbonyl)-[1,1'-biphenyl]-3-yl ester.

* Correspondence to: Faculty of Experimental Sciences, Universidad Francisco de Vitoria, UFV, Pozuelo de Alarcón, 28223 Madrid, Spain.

E-mail address: fernando.berrendero@ufv.es (F. Berrendero).

¹ Present address: Pharmacology Unit, Department of Pathology and Experimental Therapeutics, Neurosciences Institute, University of Barcelona and Bellvitge University Hospital-IDIBELL, 08908L'Hospitalet de Llobregat, Spain.

<https://doi.org/10.1016/j.bioph.2022.112925>

Received 21 January 2022; Received in revised form 25 March 2022; Accepted 4 April 2022

Available online 9 April 2022

0753-3322/© 2022 The Author(s). Published by Elsevier Masson SAS. This is an open access article under the CC BY-NC-ND license (<http://creativecommons.org/licenses/by-nc-nd/4.0/>).

1. Introduction

Orexin-A/hypocretin-1 (OXA) and Orexin-B/hypocretin-2 (OXB) are neuropeptides of the lateral hypothalamus that project throughout the brain [1,2] and bind two G protein-coupled receptors, orexin receptor-1 (OX1R) and (OX2R) [1,2]. The orexin system is involved in diverse physiological functions including fear regulation [3,4], consistent with the existence of orexin neuronal projections to several limbic areas [5].

Pharmacological blockade or genetic deletion of OX1R impaired contextual and cued fear conditioning [6–9] in rodents. Moreover, OX1R antagonism facilitated fear extinction consolidation [8,10,11], while OXA administration impaired this response [8]. Accordingly, the activity of orexin neurons was negatively correlated with successful extinction of conditioned fear in rats [12]. Reactivity to CO₂ was significantly predictive of orexin activity in the lateral hypothalamus, and in turn high orexin activity was associated with poor extinction [13]. In humans, several studies have also described a relationship between orexins and fear and anxiety. Individuals with narcolepsy, a condition associated with a loss of orexin neurons [14], showed reduced amygdala activity and failed to acquire fear memory during aversive conditioning [15]. Patients with panic anxiety have elevated levels of OXA in the cerebrospinal fluid (CSF) [16]. However, a clinical study showed a reduction of OXA levels in the CSF and plasma of combat veterans with chronic PTSD and these levels were negatively correlated with PTSD severity [17]. Recently, an interaction between genetic polymorphisms of the OX1R and ghrelin genes was shown to affect PTSD symptom severity [18].

The endocannabinoid system (ECS), composed of two main receptors, the cannabinoid type-1 and type-2 receptors (CB1R and CB2R, respectively), their ligands, i.e. the endocannabinoids anandamide (AEA) and 2-arachidonoylglycerol (2-AG), and the enzymes involved in endocannabinoid metabolism [19] is an important neuromodulatory system crucial for appropriate fear extinction [20]. AEA through CB1R activation in the basolateral amygdala (BLA) facilitates fear extinction [21,22]. However, the role played by 2-AG in this response is less evident, and it has been suggested that an optimal level of this endocannabinoid is required for appropriate processing of fear responses [23, 24]. Several reports have described the existence of functional interactions between orexins and 2-AG, mainly in the regulation of nociception, reward and food intake [25,26]. However, whether the ECS is part of the neurobiological substrates underlying the modulation that orexins exert on fear remains to be clarified.

In this study, we investigated the participation of the ECS in the fear extinction deficits induced by orexin-A. Understanding the neurobiological mechanisms involved in these effects is essential to identify novel targets for the treatment of anxiety disorders characterized by pathological fear.

2. Material and methods

2.1. Animals

Experiments were performed using male C57BL/6 J mice (Jackson Laboratories) and the recently characterized eGFP-CB2R mice (generated by Dr. Julián Romero and Dr. Cecilia J. Hillard) and their wild-type controls (8–12 weeks old) [27]. eGFP-CB2R mice result in the expression of the enhanced green fluorescent protein (eGFP) reporter gene under the control of the endogenous mouse CB2R promoter. eGFP-CB2R mice were backcrossed for at least five generations to C57BL/6 J mice. Mice were housed in cages holding a maximum of 5 mice per cage and maintained in a temperature (21.1 ± 1 °C)- and humidity ($55 \pm 10\%$)-controlled room. Mice implanted with unilateral or bilateral cannulae were individually housed to avoid cannulae shifting or removal. Food and water were available ad libitum. Light/dark cycles were maintained in 12 h light/dark cycles (light on at 8:00 AM and off at 8:00 PM). All experiments were performed during the light phase. Mice were

handled daily for 3 days before the beginning of the experiments. All behavioural experiments were performed under blind conditions. Experimental procedures were conducted in the animal facilities of Universidad Francisco de Vitoria in Madrid, Spain, in accordance with the guidelines of the European Communities Directive 2010/63/EU and the Spanish Regulations RD 1201/2005 and 53/2013 regulating animal research and approved by the local ethical committee (CEEA-UFV).

2.2. Drugs

OXA (synthesized by Dr. David Andreu, Proteomics and Protein Chemistry, UPF, Barcelona) was dissolved in physiological saline and administered by intracerebroventricular (i.c.v.) route at $0.75 \text{ nmol} \cdot \mu\text{l}^{-1}$ or intra-BLA ($0.375 \text{ nmol} / 0.5 \mu\text{l} / \text{side}$). This dose was based on previous studies [8]. The FAAH inhibitor URB597 ($3 \text{ mg} \cdot \text{kg}^{-1}$) (Sigma) and the MAGL inhibitor JZL184 ($8 \text{ mg} \cdot \text{kg}^{-1}$) (Tocris), dissolved in physiological saline and in a solution of 15% dimethyl sulfoxide (DMSO), 5% Tween and 80% saline respectively, were administered by intraperitoneal (i.p.) route ($5 \text{ ml} \cdot \text{kg}^{-1}$ body weight). The DAGL inhibitor O7460 (synthesized by Dr. Vincenzo Di Marzo, Pozzuoli, Italy) was dissolved in 10% DMSO and 90% saline, and a volume of $1 \mu\text{l}$ was administered i.c.v. at $1 \mu\text{g} \cdot \mu\text{l}^{-1}$. The CB1R and CB2R antagonists, rimonabant ($0.1, 0.5$ and $1 \text{ mg} \cdot \text{kg}^{-1}$) (Tocris) and AM630 ($0.5, 3$ and $5 \text{ mg} \cdot \text{kg}^{-1}$) (Sigma) respectively, were administered i.p. ($10 \text{ ml} \cdot \text{kg}^{-1}$ body weight). Rimonabant was dissolved in a solution of 5% ethanol, 5% cremophor and 90% saline. AM630 was dissolved in a solution of 10% DMSO, 10% Tween 80% and 80% saline for i.p. and in DMSO/saline (2:1) for intra-BLA infusion ($3 \mu\text{g} / 0.5 \mu\text{l} / \text{side}$). The CB2R agonist JWH133 ($2 \text{ mg} \cdot \text{kg}^{-1}$) (Tocris) was dissolved in a solution of 10% DMSO, 10% Tween 80% and 80% saline, and administered by i.p. route ($10 \text{ ml} \cdot \text{kg}^{-1}$ body weight). This dose was based on previous studies [28]. Ketamine hydrochloride ($7.5 \text{ mg} \cdot \text{kg}^{-1}$) and dexmedetomidine hydrochloride ($0.5 \text{ mg} \cdot \text{kg}^{-1}$) were mixed and dissolved in saline, and administered i.p. ($6 \text{ ml} \cdot \text{kg}^{-1}$ body weight).

2.3. Behavioural experiments

2.3.1. Contextual fear conditioning and extinction

Mice were contextually fear-conditioned as performed in preceding experiments and based on previous results of our group [8,10]. The test chamber (LE116, Panlab) was made with black methacrylate walls and a transparent front door. This chamber ($25 \times 25 \times 25 \text{ cm}$) was located inside a soundproof module with a ventilation fan in order to provide a background noise and attenuate surrounding sounds. The chamber floor was constructed of parallel stainless-steel bars of 2 mm of diameter spaced at 6 mm intervals and was connected to a scrambled shock generator (LE100–26 module, Panlab). A high-sensitivity weight transducer (load cell unit) was used to record and analyse the signal generated by the animal movement intensity. Experimental software PACKWIN V2.0 automatically calculated the percentage of immobility time for each experimental phase. Before each trial, the chamber floor and walls were cleaned with 70% ethanol and then water to avoid olfactory cues. On the conditioning session, mice were individually placed in the chamber during 180 s before the exposure to the first unconditioned stimulus (US) in the absence of any stimulus to habituate mice to the new environment. After the US (0.7 mA footshock for 1 s), mice were left for 60 s to associate the US with the conditioned stimulus. A second shock was given and then mice remained in the chamber for additional 60 s. Fear extinction trials (E1–E5) were performed 24, 48, 72, 96 and 120 h after the conditioning day.

To study the consolidation of fear extinction, pharmacological treatments were administered immediately after the extinction session, except OXA which was administered 20 min later. Fear memory was assessed as the percentage of time that mice spent freezing during the first 3 min of each 5-minutes trial. Freezing behaviour, a rodent's natural response to fear, was automatically evaluated and defined as complete lack of movement, except for breathing for more than 800 ms.

Data from fear extinction were expressed as percentage of freezing behaviour and as area under the curve (AUC). AUC was calculated by using a standard trapezoid method, $AUC = [0.5 \times (B1 + B2) \times h] + [0.5 \times (B2 + B3) \times h] + \dots + [0.5 \times (Bn + Bn+1) \times h]$, where Bn were the percentage of freezing behaviour for each mouse and h was the time (days) passed between the consecutive measurements. Biochemical studies were carried out after the second extinction trial.

2.3.2. Locomotor activity

Locomotor activity was evaluated as previously reported [8]. Changes in locomotor activity were assessed by using locomotor activity boxes (27 × 27 × 21 cm, Cibertec). Mice were placed in locomotor cages with low luminosity. Activity was measured as the total number of infrared beams crossed by the animal every 5 min for 20 min.

2.4. Stereotaxic surgery and infusion procedure

Surgical procedures for i.c.v. infusion of OXA and intra-BLA administration of AM630 and OXA were performed as previously reported [8].

2.4.1. Intracerebroventricular infusion

Mice were anesthetized with a ketamine/dexmedetomidine mixture and positioned in a stereotaxic frame (KOPF Instruments). A small hole was drilled on the left or the right side of the skull randomly and an unilateral cannula (26 gauge, Plastics One) was implanted vertically into the left/right lateral ventricle according to Paxinos and Franklin [29] (from bregma: AP, -0.20 mm; ML, +/-1.00 mm; DV, 2.25 mm). The cannula was subsequently fixed to the skull with dental cement and closed with a dummy cap (33-gauge internal cannula, Plastics One). Mice were housed individually and allowed 3 days of post-operative recovery before behavioral experiments began. Microinjection procedure of OXA (0.75 nmol- μ l) was performed by connecting the cannula of freely moving mice to an injection cannula (33-gauge internal cannula, Plastics One) connected to a polyethylene tubing (PE-20, Plastics One) attached to a 10 μ l microsyringe (Model 1701 N SYR, Cemented NDL, 26 ga, 2 in, point style 3, Hamilton Company). A total volume of 1 μ l was injected at a constant rate of 1 μ l·min by using a microinfusion pump (Harvard Apparatus, Holliston). The injection cannula was removed 1 min after OXA infusion to prevent drug reflux. After completion of the behavioral experiments, 0.05% methylene blue solution (Sigma) was infused to check the correct position of the cannula. Only those mice with correct injection sites were included in the statistical analysis.

2.4.2. Intra-amygdala microinjection

Stereotaxic surgery was performed as explained above. Bilateral guide cannulae (26 gauge, Plastics One) were implanted vertically into the basolateral amygdala (BLA) according to Paxinos and Franklin [29] (from bregma: AP, -1.70 mm; ML, +/-3.35 mm; DV, -3.00 mm). Microinjections of AM630 (3 μ g/0.5 μ l/side) and OXA (0.375 nmol//0.5 μ l/side) were performed by inserting an injection cannula (33 gauge, Plastics One) into the guide cannula, which extended 1 mm beyond to reach the BLA. Drugs and vehicles were delivered at a constant rate of 0.5 μ l·min⁻¹ during 1 min. Injection cannula was removed from the guide cannula 1 min after infusion to prevent drug reflux. After completion of the behavioral experiments, coronal sections of each brain were stained with toluidine blue and the injection sites were histologically verified to be within the BLA. Only those mice with correct injection sites were included in the statistical analysis.

2.5. Measurement of endocannabinoid levels

Endocannabinoid quantification was performed as previously reported [30]. Tissues were homogenized in 5 vol of chloroform/methanol/Tris-HCl 50 mM (2:1:1) containing 1 pmol of d8-anandamide (AEA) and d5-2-arachidonoylglycerol (2-AG).

Deuterated standards were synthesized from d8-arachidonic acid and ethanolamine or glycerol, or from d4-ethanolamine. Homogenates were centrifuged at 13,000 g for 16 min (4 °C), the aqueous phase plus debris were collected and extracted again twice with 1 vol of chloroform. The organic phases from the three extractions were pooled and the organic solvents evaporated in a rotating evaporator. Lyophilized extracts were resuspended in chloroform/methanol 99:1 by vol. The solutions were then purified by open bed chromatography on silica. Fractions eluted with chloroform/methanol 9:1 by vol. (containing AEA and 2-AG) were collected and the excess solvent evaporated with a rotating evaporator, and aliquots analyzed by isotope dilution-liquid chromatography/atmospheric pressure chemical ionization/mass spectrometry (LC-APCI-MS) and allowing the separations of 2-AG and AEA. MS detection was carried out in the selected ion monitoring mode using m/z values of 356 and 348 (molecular ion +1 for deuterated and undeuterated AEA), and 384.35 and 379.35 (molecular ion +1 for deuterated and undeuterated 2-AG). Values were expressed as pmol or fmol per mg of lipid extract.

2.6. Quantitative RT-PCR analysis

Amygdala, prefrontal cortex and hippocampus tissues were extracted 10 min after the end of the extinction trial and immediately frozen at -80°C. Total RNA was purified with the RiboPure™ Kit (Invitrogen) for amygdala and prefrontal cortex, and the RNeasy Mini Kit (QIAGEN) for hippocampus, according to the manufacturer's instructions. Reverse transcription was performed with 0.8 μ g of total RNA and the SuperScript™ II Reverse Transcriptase (Invitrogen). PCR reactions were conducted using PrimePCR™ Probe Assay (Bio-Rad) to quantify mRNA levels for DAGL α (Unique Assay ID: qMmuCIP0032590), MAGL (Unique Assay ID: qMmuCIP0042348), NAPE-PLD (Unique Assay ID: qMmuCIP0035707), FAAH (Unique Assay ID: qMmuCEP0055480), CB1R (Unique Assay ID: qMmuCEP0038879), CB2R (Unique Assay ID: qMmuCEP0039299) and CX3CR1 (Unique Assay ID: qMmuCEP0058111) using GAPDH expression (Unique Assay ID: qMmuCEP0039581) as endogenous control gene for normalization. PCR assays were carried out with the CFX Connect Real-Time PCR Detection System (Bio-Rad). The fold changes in gene expression of OXA-treated animals in comparison with controls were calculated using the 2^{- $\Delta\Delta$ Ct} method.

2.7. Tissue preparation, immunofluorescence and image analysis

Immunofluorescence was performed as previously reported [27].

2.7.1. Tissue preparation for immunofluorescence

Mice were deeply anesthetized 30 min after the extinction trial by i. p. injection of the ketamine/dexmedetomidine solution and fixed by intracardiac perfusion with cold phosphate buffer saline (PBS) followed by freshly prepared cold 4% paraformaldehyde. Then, the brain was post-fixed overnight in the same fixative and dehydrated by sequential transfer to 15% and 30% sucrose solutions. Coronal frozen sections of 30 μ m thickness were obtained in a cryostat from 0.82 to -1.82 mm relative to bregma for BLA, from 1.98 to 1.54 mm relative to bregma for prefrontal cortex and from -1.46 to -2.18 mm relative to bregma for hippocampus. Brain sections were preserved in cryoprotective solution until use.

2.7.2. Immunofluorescence

Floating brain sections were washed with tris buffer saline (TBS) before overnight incubation at 4 °C with the designated primary antibodies diluted in TBS containing 1% bovine serum albumin (BSA, Sigma) and 1% Triton X-100 (Sigma). Antibodies used in this study were chicken antibody against green fluorescent protein (GFP) (1:1500, Abcam) and rabbit polyclonal antibody to Iba1 (1:1000, Wako). After primary antibody incubations, sections were washed three times in TBS followed by incubations with designed secondary antibodies at 37 °C for

2 h. Secondary antibodies used in this study were Alexa 488-conjugated goat anti-chicken IgY and Alexa 555-conjugated goat anti-rabbit IgG (both from Invitrogen). Slices were washed three times in TBS, mounted on subbed slides, air dried, and coverslipped using Fluoromount-G (Invitrogen).

2.7.3. Image analysis

The stained sections were analysed at 10 x objective using the upright microscope Nikon 90i (Nikon and Axioimager M2, Zeiss) equipped with a DXM 1200 F camera. Images (1024×1024 pixels) were obtained by using two different laser lines (488 and 561 nm) and further analysed in ImageJ software. GFP₊ cells were counted (cells per area) in coronal sections of BLA (from -0.82 to -1.82 mm relative to bregma), prefrontal cortex (from 1.98 to 1.54 mm relative to bregma) and hippocampus (from -1.46 to -2.18 mm relative to bregma). Colocalization of GFP with microglial cells was quantified using the ImageJ manual particle counting option. The option "freehand selections" was used to limit the area of BLA and the microglial soma perimeter. For prefrontal cortex analysis, a $540 \mu\text{m}$ side square region of interest (ROI) was delimited for quantification. Four to six images per brain area of each animal were analysed.

2.8. Microglial depletion through chow treatment

The colony stimulating factor 1 receptor (CSF1R) inhibitor PLX5622 was provided by Plexxikon (Plexxikon Inc) and formulated in AIN-76A chow at dose of 1200 parts per million (Research Diets). Blockade of maintained CSF1R induces continuous microglial depletion. C57BL/6 mice received PLX5622 or control chow for 4 days after stereotaxic surgery recovery and throughout the behavioural test. The selected dose and duration of PLX5622 treatment were based on previous studies showing 80% microglial depletion with the same dose and similar treatment duration [31].

2.9. Statistical analysis

Comparisons between two groups were assessed by Student's *t* tests. Multiple-group comparisons were performed by one-way or two-way analysis of variance (ANOVA), as appropriate. Repeated-measurement ANOVA was used for serial freezing and locomotion responses. Subsequent Fisher's LSD post-hoc test was only used when ANOVA interaction effects were significant. Pearson correlation coefficient was used to analyse the strength of relationship between two variables. All data were expressed as mean \pm SEM. The statistical analysis was performed using Statistica (StatSoft) software. The level of significance was $p < 0.05$ in all experiments.

3. Results

3.1. Impairment of fear extinction induced by OXA is mediated by 2-AG

First, we evaluated the effect of 2-AG and AEA in the extinction of fear memories by inhibiting the activity of monoacylglycerol lipase (MAGL) and fatty acid amide hydrolase (FAAH), the enzymes that degrade 2-AG and AEA respectively, in a contextual fear conditioning paradigm (Fig. 1A). The MAGL inhibitor JZL184 ($8 \text{ mg}\cdot\text{kg}^{-1}$, ip), but not the FAAH inhibitor URB597 ($3 \text{ mg}\cdot\text{kg}^{-1}$, ip), significantly impaired fear extinction as showed the increase of freezing behaviour and AUC (Fig. 1B,C) when compared to the control group. Locomotor activity was not modified in mice 24 h after acute administration of JZL184 ($8 \text{ mg}\cdot\text{kg}^{-1}$, ip) (Fig. S1), demonstrating that the changes observed in freezing behaviour were not due to unspecific effects on locomotion. OX1R activation in response to OXA promotes diacylglycerol (DAG) production which in turn is used by diacylglycerol lipases (DAGL) as a substrate for 2-AG synthesis [26,32]. Interestingly, the pretreatment with the specific DAGL inhibitor O7460 ($1 \mu\text{g}\cdot\mu\text{l}^{-1}$, icv) before OXA

($0.75 \text{ nmol}\cdot\mu\text{l}^{-1}$, icv) (Fig. 1A) prevented the impairment of fear extinction induced by the neuropeptide (Fig. 1D,E). Taken together, these results suggest that OXA recruits 2-AG to regulate fear extinction.

Next, we studied whether acute OXA infusion, at the same dose that produces impairment of fear extinction, increases 2-AG levels in amygdala, prefrontal cortex and hippocampus, key brain regions related to contextual fear regulation [33]. An enhancement of 2-AG was observed in the amygdala 10 min, but not 30 min, following OXA administration (Fig. 1F). In the prefrontal cortex, 2-AG increased 30 min, but not 10 min, after OXA injection (Fig. 1G). Surprisingly, a decrease of 2-AG was found in the hippocampus 30 min after OXA infusion (Fig. 1H). There were no significant differences between saline and OXA treatment groups at 60 min (Fig. S2), while AEA levels were not modified in any brain area at the different time points analysed (Fig. S3 and S4). All together, these data suggest that OXA induces resistance to fear extinction through increased levels of 2-AG, probably in the amygdala.

3.2. Impaired fear extinction is associated with increased 2-AG levels in the amygdala and hippocampus

To further study the role played by 2-AG in the extinction deficit exerted by OXA, we measured endocannabinoid levels just before and 10 min after the second extinction session in mice treated with saline or OXA ($0.75 \text{ nmol}\cdot\mu\text{l}^{-1}$, icv) after the first extinction trial (Fig. 2A). As expected, OXA impaired fear extinction in comparison with control mice (Fig. 2B). No changes in 2-AG levels were observed between groups in any brain area before the extinction session (Fig. 2C,D,E). Notably, 2-AG levels increased in the amygdala and hippocampus (Fig. 2C,E), but not in the prefrontal cortex (Fig. 2D), after the extinction session in animals treated with OXA that do not extinguish fear (Fig. 2B). Indeed, a significant correlation between fear memory (freezing values) and 2-AG levels was observed in the amygdala (Fig. 2F). No correlation was found neither in the prefrontal cortex nor in the hippocampus (Fig. S5). OXA did not modify AEA levels analysed before and after the extinction session in any brain region (Fig. S6). These results suggest that an optimal level of 2-AG is required for appropriate processing of fear responses and that high amygdalar and hippocampal 2-AG levels induced by OXA infusion are related to extinction deficits.

3.3. Impairment of fear extinction induced by OXA is associated with increased expression of CB2R in the amygdala

Given the role played by 2-AG in the extinction deficit induced by OXA, we determined the effects of OXA ($0.75 \text{ nmol}\cdot\mu\text{l}^{-1}$, icv) on gene expression of the endocannabinoid-synthesizing and degrading enzymes, as well as CB1R and CB2R. Brain tissue was removed 10 min after the second extinction session, in OXA- or saline-treated mice after the first session. In the amygdala, OXA infusion increased the mRNA encoding for DAGL α (Fig. 3A), but not MAGL, suggesting that the enhancement of 2-AG previously observed is due to the increase in the synthesis of this endocannabinoid. However, N-acyl phosphatidylethanolamine phospholipase D (NAPE-PLD) expression, but not FAAH, was also elevated after OXA treatment (Fig. 3A), indicating that increased expression of AEA biosynthetic enzymes was not sufficient alone to cause here elevation of the levels of the corresponding endocannabinoid. Notably, quantitative RT-PCR analysis showed an increase of CB2R expression ($\sim 53\%$), but not CB1R, in the amygdala of mice treated with OXA that are resistant to fear extinction (Fig. 3A). By contrast, no changes were observed in the expression of any of these genes either in the prefrontal cortex or the hippocampus (Fig. 3B,C).

To study the specific location of the CB2R in the amygdala, we used the recently characterized eGFP-CB2R mice [27], in which the expression of enhanced green fluorescent protein (eGFP) is under the control of the endogenous mouse CB2R promoter. These mice were treated with saline or OXA ($0.75 \text{ nmol}\cdot\mu\text{l}^{-1}$, icv) after the first session trial, and brain

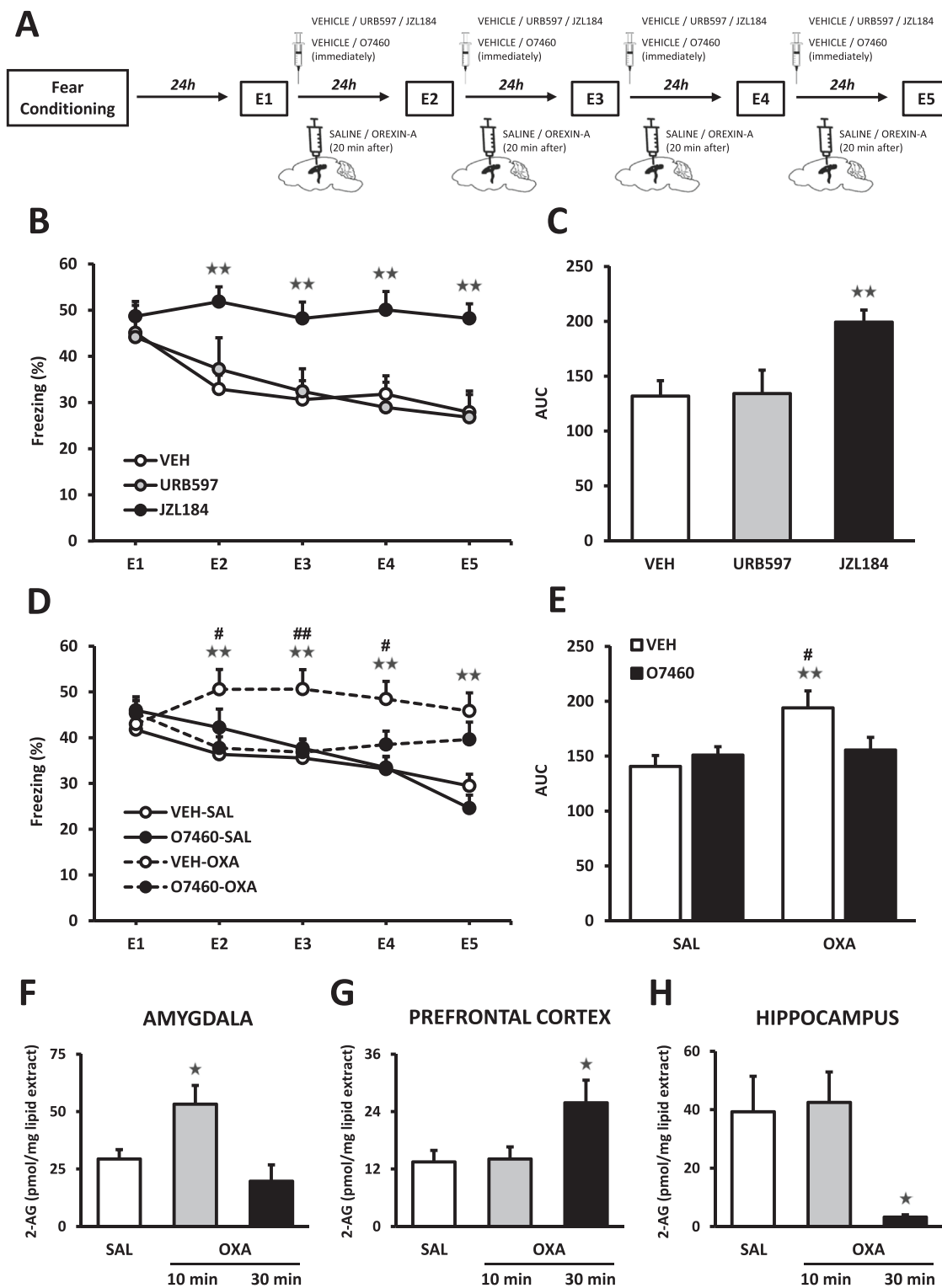


Fig. 1. Impaired fear extinction induced by OXA is modulated by 2-AG. (A) Schematic representation of the experimental design for behavioural tests. (B,C) Time course of the freezing levels during contextual extinction trials (interaction day x treatment: $F_{8,120} = 2.28$, $p < 0.05$) (B) and AUC values (treatment effect: $F_{2,30} = 7.17$, $p < 0.01$) (C) in mice treated immediately after each extinction session with JZL184 ($8 \text{ mg}\cdot\text{kg}^{-1}$, ip), URB597 ($3 \text{ mg}\cdot\text{kg}^{-1}$, ip) or VEH ($n = 8-3$ mice per group). (D,E) Time course of the freezing levels during contextual extinction trials (day x pretreatment x treatment interaction ($F_{4,128} = 3.16$, $p < 0.05$) (D) and AUC values (pretreatment x treatment interaction ($F_{1,32} = 4.11$, $p < 0.05$) (E) in mice treated with O7460 ($1 \mu\text{g}\cdot\mu\text{l}$, icv) immediately after each extinction session, 20 min before OXA ($0.75 \text{ nmol}\cdot\mu\text{l}^{-1}$, icv) infusion ($n = 8-10$ mice per group). (F,G,H) Levels of 2-AG in amygdala ($F_{2,14} = 6.56$, $p < 0.01$) (F), prefrontal cortex ($F_{2,15} = 4.26$, $p < 0.05$) (G) and hippocampus ($F_{2,15} = 5.56$, $p < 0.05$) (H), in homogenates extracted 10 and 30 min after acute OXA ($0.75 \text{ nmol}\cdot\mu\text{l}^{-1}$, icv) infusion ($n = 5-6$ mice per group). Data are expressed as mean \pm SEM. * $p < 0.05$, ** $p < 0.01$ (compared with VEH in (B,C), VEH-SAL in (D,E) and SAL in (F,G,H)); # $p < 0.05$, ## $p < 0.01$ (comparison with O7460-OXA group). OXA: orexin-A; VEH: vehicle; SAL: saline; E1-E5: extinction trials 1-5; AUC: area under the curve; 2-AG: 2-arachidonoylglycerol.

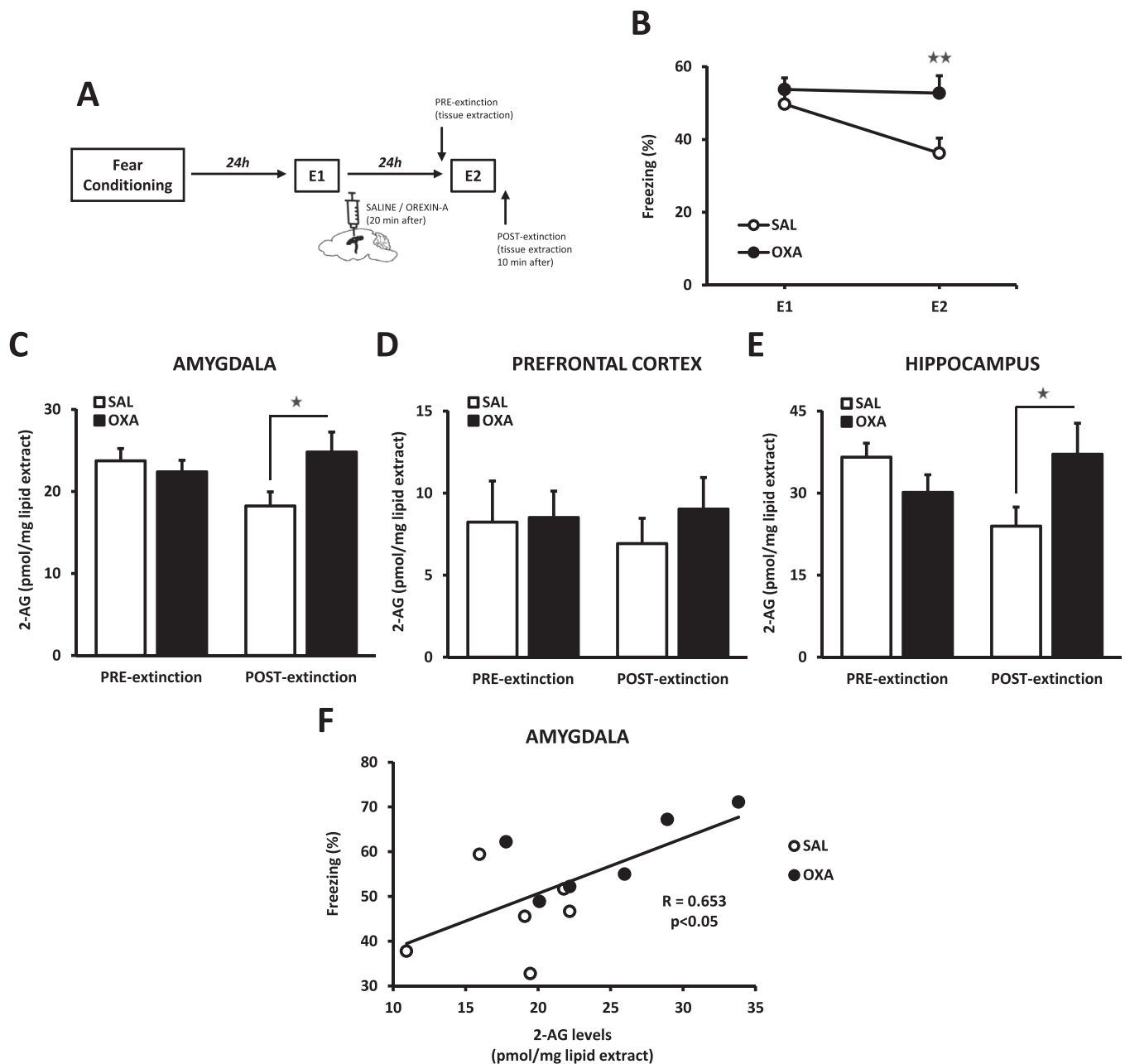


Fig. 2. High levels of 2-AG in the amygdala and hippocampus are associated with impaired fear extinction. (A) Schematic representation of the experimental design for behavioural test. OXA (0.75 nmol·μl⁻¹, icv) or SAL were injected 20 min after E1, and brain tissue was obtained immediately before or 10 min after E2. (B) Time spent freezing by SAL- and OXA-treated mice during E1 and E2 (n = 9–12 mice per group) (interaction day x treatment: F_{1,19} = 7.69, p < 0.05). (C) 2-AG levels in the amygdala before (pre-extinction) and 10 min after (post-extinction) E2 (interaction experimental condition x treatment: F_{1,20} = 4.76, p < 0.05) (n = 6 mice per group). (D) 2-AG levels in the prefrontal cortex before (pre-extinction) and 10 min after (post-extinction) E2 (n = 6 mice per group). (E) 2-AG levels in the hippocampus before (pre-extinction) and 10 min after (post-extinction) E2 (interaction experimental condition x treatment: F_{1,18} = 7.32, p < 0.05) (n = 4–6 mice per group). (F) Correlation between fear memory (freezing values) and 2-AG levels in the amygdala after E2 in mice treated with SAL or OXA 20 min following E1. Data are expressed as mean ± SEM. *p < 0.05, **p < 0.01 (compared with SAL). OXA: orexin-A; SAL: saline; E1-E2: extinction trials 1–2; 2-AG: 2-arachidonoylglycerol.

tissue was perfused 30 min after the second extinction session (Fig. 3D). Additional control mice were injected with saline or OXA and perfused 24 h later without exposing to footshock (Fig. 3D). In agreement with quantitative RT-PCR analysis, an enhancement of eGFP signal in the BLA (~29%) was found in mice infused with OXA 20 min after the first extinction session in comparison with saline-treated mice (Fig. 3E,J), suggesting an association between impaired extinction and increased eGFP (CB2R) expression. Interestingly, most of the eGFP+ cells (~80%) co-localized with Iba1, a commonly used marker of microglia (Fig. 3H, J), indicating that CB2R-dependent eGFP expression takes place mainly in microglial cells. Moreover, a significant increase in the perimeter of

microglia soma was observed in eGFP+ cells (Fig. 3I), independently of saline or OXA treatment. This result indicates that the expression of CB2R is associated with a shift of microglia morphology to a reactive state which is characterized by larger amoeboid soma [34]. No changes in eGFP signal were observed either in the prefrontal cortex or the hippocampus due to OXA infusion (Fig. 3F,G). Basal expression of CB2R was scarce as shown by the low eGFP immunoreactivity in mice that were not exposed to footshock, in the different brain areas evaluated (Fig. 3E,F,G). Moreover, OXA administration by itself did not modify CB2R expression (Fig. 3E,F,G). Taken together, these data suggest that fear extinction deficits induced by OXA are associated with increased

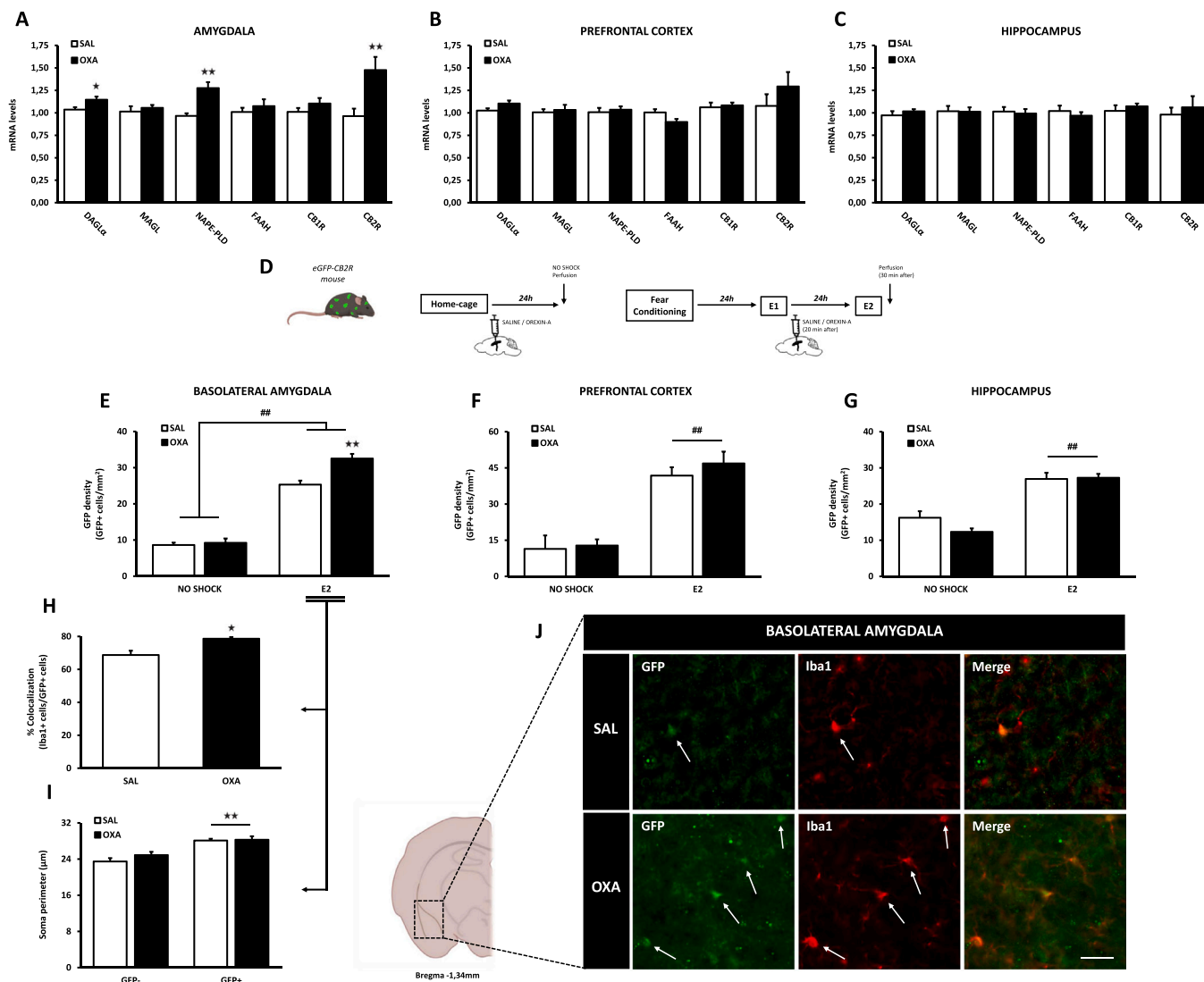


Fig. 3. Impaired fear extinction induced by OXA is associated with increased expression of CB2R in the amygdala. (A,B,C) Gene expression of the endocannabinoid synthesizing and degrading enzymes, CB1R and CB2R in amygdala (A), prefrontal cortex (B) and hippocampus (C) 10 min after E2 in mice treated with SAL or OXA (0.75 nmol·µl, icv) 20 min following E1 (n = 8–12 mice per group). (D) Schematic representation of the experimental design for (E–I) biochemical experiments. (E,F, G) GFP staining in the basolateral amygdala (interaction experimental condition x treatment: $F_{1,11} = 7.59$, $p < 0.05$) (E), prefrontal cortex (experimental condition: $F_{1,10} = 43.89$, $p < 0.001$) (F) and hippocampus (experimental condition: $F_{1,10} = 76.28$, $p < 0.001$) (G) of eGFP-CB2R mice injected with SAL or OXA and sacrificed 24 h later without receiving footshock, and mice exposed to fear conditioning and sacrificed 30 min after E2, treated with SAL or OXA 20 min following E1 (n = 4–5 mice per group). (H) Percentage of GFP+ cells expressing Iba1 in the basolateral amygdala of eGFP-CB2R mice after E2, treated with SAL or OXA 20 min following E1 (n = 4–5 mice per group). (I) Soma perimeter of microglia in GFP+ and GFP- cells in the basolateral amygdala of eGFP-CB2R mice sacrificed after E2, treated with SAL or OXA 20 min following E1 (eGFP effect: $F_{1,14} = 37.35$, $p < 0.01$) (n = 4–5 mice per group). (J) Representative images of the basolateral amygdala of eGFP-CB2R mice labelling GFP (green), Iba1 (red) and colocalization of GFP and Iba1. The scale bar represents 20 µm. Data are expressed as mean ± SEM. * $p < 0.05$, ** $p < 0.01$ (compared with SAL or GFP- cells); ## $p < 0.01$ (compared with NO SHOCK group). OXA: orexin-A; SAL: saline; E1-E2: extinction trials 1–2.

expression of CB2R in microglial cells of the BLA.

3.4. CB2R mediates the impairment of fear extinction induced by OXA

2-AG is a full agonist of CB1R and CB2R [35]. Therefore, in view of the role played by 2-AG in the impairment of fear extinction induced by OXA, we studied the cannabinoid receptor subtype involved in this effect. A low dose of the CB1R antagonist rimonabant (0.5 mg·kg⁻¹, ip) (Fig. 4A) was used to rule out an intrinsic effect of this cannabinoid ligand. Interestingly, pretreatment with rimonabant potentiated the resistance of fear extinction induced by OXA (0.75nmol·µl⁻¹, icv) (Fig. 4B,C). On the contrary, blockade of the CB2R with the specific antagonist AM630 (3 mg·kg⁻¹, ip) (Fig. 4D) completely prevented the extinction deficit induced by OXA (Fig. 4E,F). Locomotor activity was

not modified in mice 24 h after acute administration of OXA (0.75nmol·µl⁻¹, icv), rimonabant (0.5 mg·kg⁻¹, ip), and AM630 (3 mg·kg⁻¹, ip) (Fig. S7). Pretreatment with rimonabant or AM630 before OXA also did not alter locomotion 24 h later (Fig. S7). Moreover, rimonabant injection (0.5 mg·kg⁻¹, ip) before OXA (0.75nmol·µl⁻¹, icv) during four days did not induce changes in locomotor activity measured 24 h after the last administration day (fifth day) (Fig. S8). These data demonstrate that the changes observed in freezing behaviour were not due to unspecific effects on locomotion. As a whole, these results are in agreement with the increased expression of CB2R previously observed in the BLA of mice treated with OXA. Moreover, the potentiation of the extinction deficits induced by the per se inactive dose of rimonabant could reflect a blockade of a compensatory and/or simultaneous facilitation of fear extinction through activation of CB1Rs.

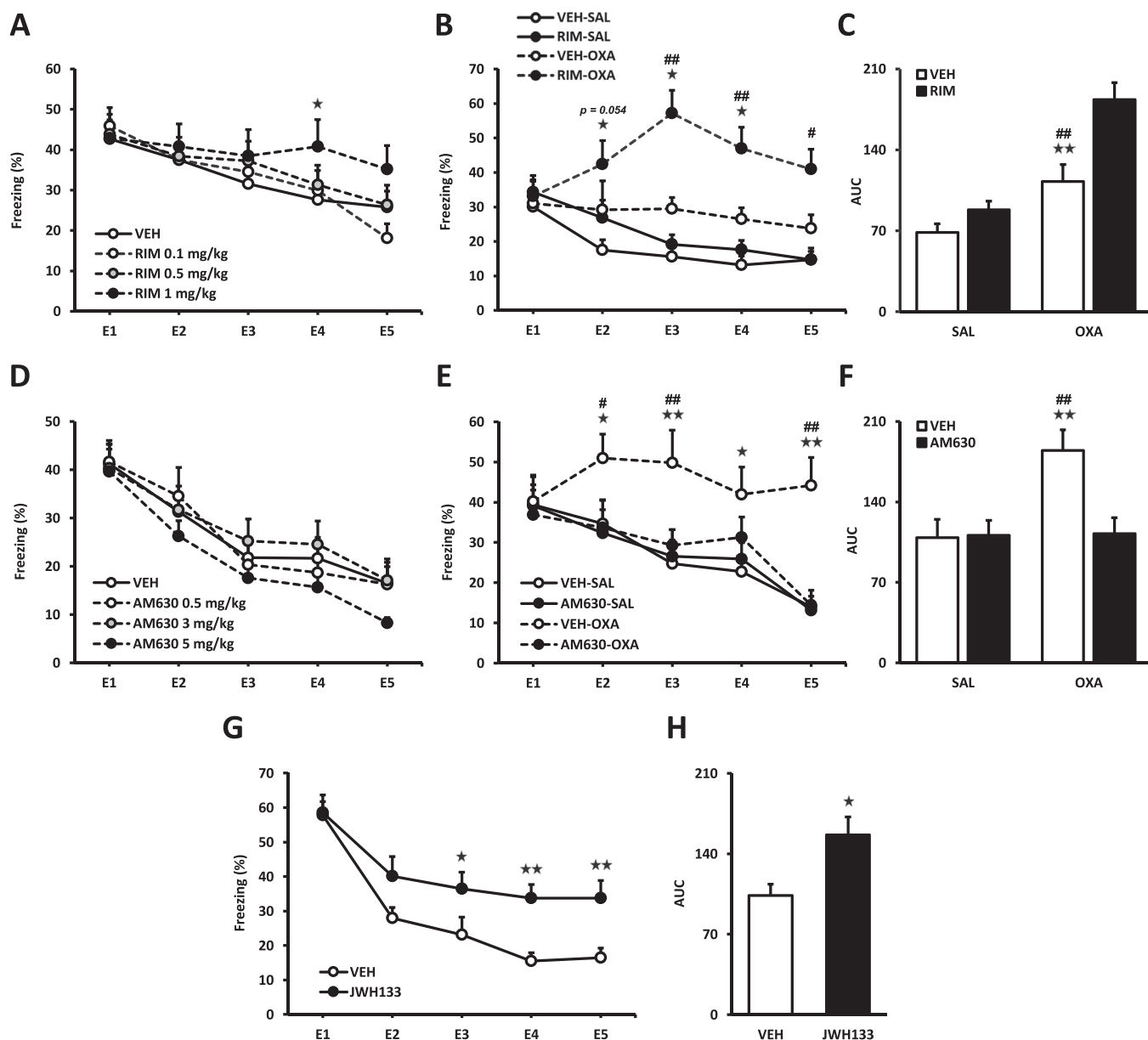


Fig. 4. Impaired fear extinction induced by OXA is mediated by CB2R. (A,D) Time course of the freezing levels during contextual extinction trials in mice treated with the CB1R antagonist rimonabant (0.1, 0.5 and 1 mg·kg⁻¹, ip) (A) or the CB2R antagonist AM630 (0.5, 3 and 5 mg·kg⁻¹, ip) (D) immediately after each extinction session (n = 12–24 mice per group). (B,C,E,F) Time course of the freezing levels during contextual extinction trials (interaction pretreatment x treatment: F_{1,35} = 4.53, p < 0.05) (B), (interaction pretreatment x treatment: F_{1,38} = 5.80, p < 0.05) (E) and AUC values (interaction pretreatment x treatment: F_{1,35} = 5.28, p < 0.05) (C), (interaction pretreatment x treatment: F_{1,38} = 5.78, p < 0.05) (F) in mice treated with rimonabant (0.5 mg·kg⁻¹, ip) (n = 7–12 mice per group) (B,C) or AM630 (3 mg·kg⁻¹, ip) (n = 9–11 mice per group) (E,F) immediately after each extinction session, 20 min before OXA (0.75 nmol·μl⁻¹, icv) infusion. (G,H) Time course of the freezing levels during contextual extinction trials (day x treatment interaction: F_{4,88} = 2.27, p < 0.05) (G) and AUC values (H) in mice treated with the CB2R agonist JWH133 (2 mg·kg⁻¹, ip) immediately after each extinction session (n = 11–13 mice per group). Data are expressed as mean ± SEM. *p < 0.05, **p < 0.01 (compared with VEH or SAL); #p < 0.05, ##p < 0.01 (comparison between pretreatments). OXA: orexin-A; VEH: vehicle; SAL: saline; E1-E5: extinction trials 1–5; AUC: area under the curve.

Given that CB2Rs underpin the fear extinction deficits of OXA, as suggested by their blockade by AM630, direct-acting CB2R agonists should also promote fear extinction resistance. Accordingly, the CB2R agonist JWH133 (2 mg·kg⁻¹, ip), administered immediately after each extinction session, impaired fear extinction (Fig. 4G,H), confirming a novel functional role for CB2R in the modulation of fear extinction.

3.5. Intra-amygdala infusion of the CB2R antagonist AM630 prevents the fear extinction deficits promoted by OXA

Considering the behavioural and biochemical data previously

described, we next evaluated the possible direct participation of CB2Rs located in the amygdala in the extinction deficits induced by OXA. For this purpose, mice were bilaterally implanted with cannulae into the BLA and received intra-structure microinjections of AM630 (3 μg/0.5 μl/side) immediately after each contextual extinction session and OXA (0.375 nmol/0.5 μl/side) 20 min later. Notably, pretreatment with AM630 into the BLA completely blocked the impaired fear extinction induced by intra-BLA infusion of OXA (Fig. 5A,B). Representative location of the injection sites and a characteristic image of bilateral cannulae positions (Fig. 5C,D) are shown. This result demonstrates an unequivocal role for amygdalar CB2R in the impaired fear extinction

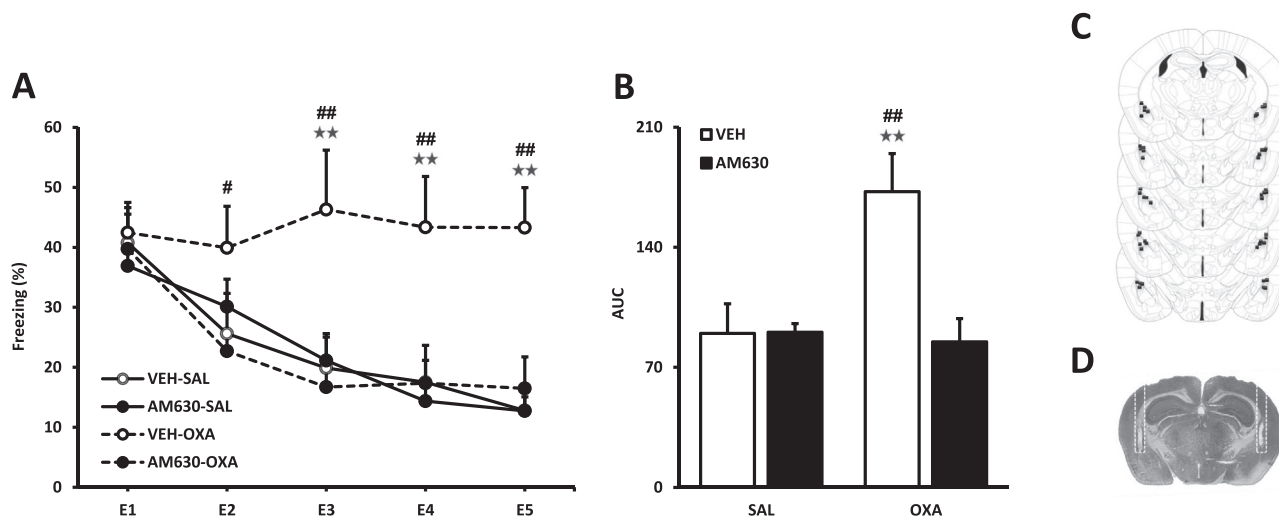


Fig. 5. Intra-amygdala infusion of the CB2R antagonist AM630 blocks the impaired fear extinction induced by intra-amygdala administration of orexin-A. Mice were bilaterally cannulated in the BLA, and after recovery were subjected to contextual fear conditioning and extinction procedure. (A,B) Time course of the freezing levels during contextual extinction trials (interaction pretreatment \times treatment: $F_{1,28} = 7.33$, $p < 0.05$) (A), and AUC values (interaction pretreatment \times treatment: $F_{1,28} = 7.79$, $p < 0.01$) (B), in mice treated with AM630 ($3 \mu\text{g}/0.5 \mu\text{l}/\text{side}$) immediately after each extinction session, 20 min before OXA ($0.375 \text{nmol}/0.5 \mu\text{l}/\text{side}$) infusion ($n = 8$ mice per group). (C) Schematic representation of microinjections sites within the BLA. The number of dots in the figure is fewer than the actual number of animals used because of data overlapping. (D) Photomicrograph of a coronal section of a representative subject showing bilateral injection sites within the mice BLA. Data are expressed as mean \pm SEM. $^{**}p < 0.01$ (compared with VEH or SAL); $\#p < 0.05$; $\#\#p < 0.01$ (comparison between pretreatments). OXA: orexin-A; VEH: vehicle; SAL: saline; E1-E5: extinction trials 1–5; AUC: area under the curve.

promoted by OXA.

3.6. Microglial depletion blocks the increase of CB2R expression in the amygdala and prevents the impairment of fear extinction induced by OXA

To determine the contribution of amygdalar CB2R located in microglial cells in the fear extinction deficit induced by OXA, we used PLX5622, a colony-stimulating factor-1 receptor (CSF1R) antagonist, to pharmacologically deplete microglia in animals undergoing the fear extinction process. To this aim, 4 days before starting behavioural evaluation, both saline- and OXA-treated mice were given either control chow or PLX5622 chow (Fig. 5A). Notably, the impairment of fear extinction induced by OXA ($0.75 \text{nmol} \cdot \mu\text{l}^{-1}$, icv) was totally prevented in mice exposed to PLX5622 chow (Fig. 5B,C). PLX5622 chow exposure during four days did not modify locomotor activity evaluated 24 h later (Fig. S1). In agreement with previous reports [31,36], microglia were successfully deleted in the amygdala as shown by the dramatic decrease in the expression of the microglial marker CX3CR1 ($\sim 80\%$) by quantitative RT-PCR analysis in saline and OXA-treated mice exposed to PLX5622 chow (Fig. 5D). Moreover, the enhanced expression of CB2R in the amygdala of mice infused with OXA and exposed to control diet that are resistant to fear extinction was markedly decreased ($\sim 80\%$) due to PLX5622 chow exposure (Fig. 5E). However, as previously observed, mRNA expression of CB1R was not affected by either OXA infusion or by PLX5622 chow treatment (Fig. 5F). These data suggest that CB2Rs located in microglial cells of the amygdala may be involved in the fear extinction deficits induced by overactivation of the orexin system. (Fig. 6).

4. Discussion

Our data demonstrate a pivotal role for 2-AG in the impairment of fear extinction induced by OXA. Moreover, we reveal that CB2Rs, specifically those located in the amygdala, are involved in the extinction deficit triggered by OXA.

Orexins are implicated in the modulation of emotional behaviours [3,4], and activation of this system is related to poor extinction of conditioned fear. In humans, patients with panic anxiety symptoms

show elevated CSF orexin concentrations [16]. Consistent with this, OX1R blockade facilitated fear extinction in animal models [8,11] and reduced CO₂-induced fear and anxiety symptoms in humans [37]. A better understanding of the neurobiological mechanisms by which orexins regulate fear extinction may provide novel pharmacologic targets for PTSD or panic disorders.

OXA triggers biosynthesis of the endocannabinoid 2-AG via the PLC/DAG/DAGL α pathway downstream to OX1R [25], a Gq-protein-coupled receptor. Functional interactions between orexins and endocannabinoids have been reported, mainly in the regulation of pain [38–40], food intake [41,42], and cocaine relapse [43]. A general mechanism of these interactions implies OXA-induced synthesis of 2-AG and subsequent CB1R-dependent retrograde inhibition of GABA release, leading to disinhibition of different pathways in brain areas such as the periaqueductal grey matter [38] or the ventral tegmental area [43].

We investigated the possible involvement of 2-AG in the fear extinction deficit induced by OXA given that the ECS also plays an important role in the modulation of the extinction of aversive memories [20,21]. O7460, a selective inhibitor of DAGLs [44], which are the enzymes in charge of 2-AG biosynthesis, prevented the impaired fear extinction elicited by OXA. Consistently, an early increase of 2-AG, but not AEA, was observed in the amygdala after the infusion of OXA at the same dose that impairs extinction. At a later time point, 2-AG levels increased in the prefrontal cortex, maybe due to an indirect effect of OXA rather than direct orexin-mediated stimulation of 2-AG biosynthesis. Intriguingly, the levels of 2-AG dramatically decreased in the hippocampus at the same later time point. OXA administration could modify, through the alteration of 2-AG levels, the communication between these brain regions that underlies important cognitive and behavioural functions [45]. Indeed, the ECS is a fundamental regulator in synaptic plasticity and functional connectivity in the hippocampus-prefrontal cortex pathway [46].

Our data also demonstrate that high levels of 2-AG are related to resistance of fear extinction. Thus, 2-AG levels increased in the amygdala and the hippocampus, but not in the prefrontal cortex, after the extinction session in mice treated with OXA that did not extinguish fear. A significant correlation between fear memory (freezing values) and 2-AG levels was also found in the amygdala. Moreover, in agreement with

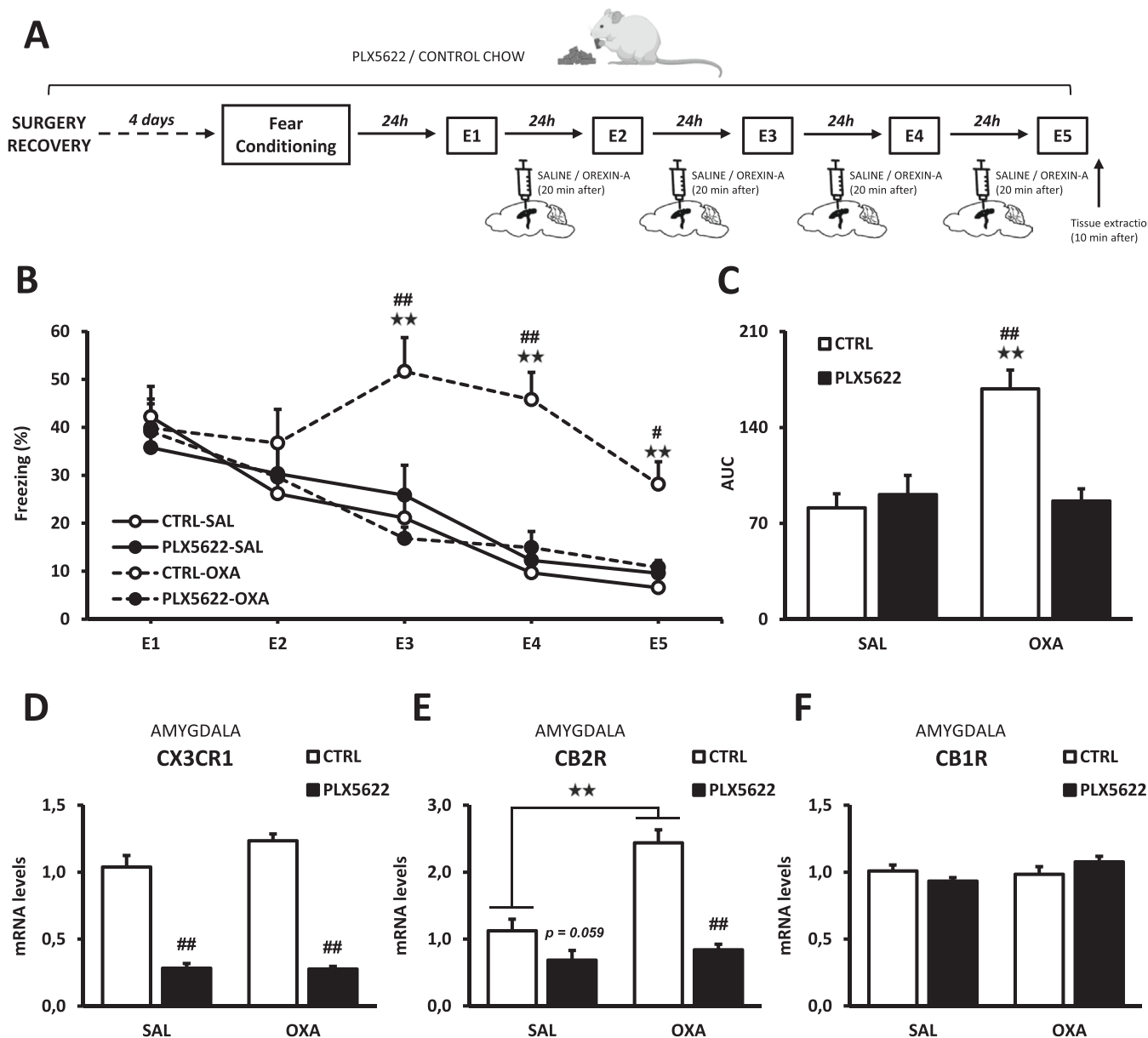


Fig. 6. Microglial and CB2R depletion in the amygdala with PLX5622 chow prevents the impairment of fear extinction induced by OXA. (A) Schematic representation of the experimental design. (B,C) Time course of the freezing levels during contextual extinction trials (interaction day x diet x treatment: $F_{4,152} = 3.78$, $p < 0.01$) (B) and AUC values (interaction diet x treatment: $F_{1,38} = 14.77$, $p < 0.001$) (C) in mice treated with SAL or OXA ($0.75 \text{ nmol} \cdot \mu\text{l}^{-1}$, icv) 20 min after each extinction session, and exposed to control or PLX5622 chow ($n = 10\text{--}11$ mice per group). (D-F) Gene expression of CX3CR1 (diet effect: $F_{1,31} = 204.81$, $p < 0.001$) (D), CB2R (interaction diet x treatment: $F_{1,30} = 13.28$, $p < 0.01$) (E), and CB1R (F) in the amygdala of mice treated with SAL or OXA ($0.75 \text{ nmol} \cdot \mu\text{l}^{-1}$, icv) 20 min after each extinction session, and exposed to control or PLX5622 chow. Tissue was extracted 10 min after the last extinction session ($n = 7\text{--}10$ mice per group). Data are expressed as mean \pm SEM. ** $p < 0.01$ (compared with SAL); # $p < 0.05$, ## $p < 0.01$ (comparison between diets). OXA: orexin-A; CTRL: control diet; SAL: saline; E1-E5: extinction trials 1–5; AUC: area under the curve.

previous reports [23], the administration of JZL184, an inhibitor of MAGL which is responsible for 2-AG degradation, impaired fear extinction. Therefore, an optimal level of 2-AG could be required for appropriate processing of fear responses since mice deficient in DAGL α , which have reduced 2-AG brain levels, also exhibit impaired fear extinction [47]. This is feature also of germ-free mice [48], which are also characterised by lower brain 2-AG levels [49]. On the other hand, CB1R knockout mice and wild-type mice treated with the CB1R antagonist rimonabant show resistance to fear extinction [21] and consistently, AEA facilitates fear extinction by CB1R activation in the BLA [22]. Taken together, these data suggest potentially opposing functions of AEA and 2-AG on fear extinction modulation indicating that endocannabinoid signalling could play a more complex role in the regulation

of fear learning processes than previously thought.

We next explored the cannabinoid receptor subtype involved in the mediation exerted by 2-AG in OXA-induced impaired fear extinction given that this endocannabinoid, unlike AEA, is a full agonist at CB1R and CB2R [35]. In this study we propose that CB2Rs located in the amygdala are involved in the fear extinction deficit produced by OXA infusion. This proposal is based on the following observations: (i) mRNA levels of CB2R increased in the amygdala, but not in the prefrontal cortex or the hippocampus, in mice treated with OXA and resistant to fear extinction. Importantly, a similar increase of CB2R was observed in the BLA by using eGFP-CB2R mice. Most of CB2Rs colocalized with microglial cells, which were activated by the presence of this cannabinoid receptor subtype; (ii) systemic and intra-BLA CB2R antagonism

with AM630 completely prevented the extinction deficit of OXA; (iii) administration of the selective CB2R agonist, JWH133, induced impairment of fear extinction; (iv) microglia depletion in the amygdala following exposure to PLX5622 chow reduced the increased expression of CB2R in OXA-treated mice, and suppressed the extinction deficit induced by the neuropeptide, suggesting a participation of CB2Rs located in microglial cells of the amygdala in this effect. Conversely, CB1R mRNA was not altered by microglia reduction, consistent with the main localization of this receptor in neurons.

Although the CB2R was initially regarded as a peripheral cannabinoid receptor, several studies indicate that this receptor is expressed in the CNS mainly under pathological conditions. Thus, brain CB2Rs are highly inducible in response to various insults [50–53] and have been involved in the regulation of different neurobiological processes including cognition, and mood-related (anxiety, depression) behaviours [54]. A recent study has shown an anxiolytic-like effect of 2-AG through CB2R activation in a model of innate predator-induced fear [53]. While evidence for a role of CB2R in anxiolytic-like effects is still sparse, MAGL inhibition has emerged as a potential target for anxiolytic drug discovery [55]. However, based on our data and as previously suggested [23], 2-AG signalling and CB2R could play a different role in the modulation of unconditioned anxiety and stress responses versus conditioned fear behaviours, emphasizing the complexity of the ECS involvement in emotional regulation. It is noteworthy that, while deletion of CB2R was found to disrupt the consolidation of foot-shock aversive memories using the step-down inhibitory avoidance test [56], the possible involvement of CB2R in fear extinction learning has not been previously reported. The apparent opposing role for CB1R and CB2R in the regulation of fear extinction could explain why unselective activation of cannabinoid receptors by, e.g., cannabis preparations or Δ^9 -tetrahydrocannabinol, has so far been found of controversial efficacy [57,58] to treat these disorders, despite the beneficial role played therein by CB1Rs.

Our data reveal that the impairment of fear extinction induced by the overactivation of the orexin system is mediated by 2-AG and amygdalar CB2R stimulation. Moreover, although the intervention of other cell types cannot be ruled out, our results suggest that microglial cells of the amygdala could be responsible of this effect. A growing body of evidence demonstrates that CB2R is up-regulated in microglia in the context of neuroinflammatory diseases [59]. Given the presence of CB2R in activated microglial cells of the amygdala during the extinction process, future experimental work will be necessary to elucidate the consequences of CB2R-mediated microglial activation during fear extinction. Indeed, altered microglial function and inflammation may contribute to fear dysregulation [60], and has been suggested to underlie the impairment of fear extinction in germ-free or antibiotic-treated mice [48]. Levels of the proinflammatory cytokine TNF α increased in microglia from mice during retention of fear memory [61] while altered blood concentrations of cytokine such as IL6, IL1 β or TNF α were associated with PTSD disorder in humans [62].

5. Conclusions

In summary, our multidisciplinary study revealed the involvement of 2-AG and CB2R located in the amygdala in the impaired fear extinction induced by overactivation of the orexin system. In addition, based on our biochemical and behavioural data, microglial CB2Rs in this brain area seem to be involved in this effect, although this statement needs to be confirmed by further research. The discovery of this novel mechanism warrants the study of new approaches in the treatment of disorders characterized by pathological fear.

CRedit authorship contribution statement

Marc Ten-Blanco: Conceptualization, Data curation, Formal analysis, Investigation, Methodology, Validation, Writing – original draft,

Writing – review & editing; **África Flores:** Conceptualization, Formal analysis, Investigation, Methodology, Writing- original draft; **Inmaculada Pereda-Pérez:** Data curation, Formal analysis, Investigation, Methodology, Writing – original draft; **Fabiana Piscitelli:** Investigation, Methodology; **Cristina Izquierdo-Luengo:** Formal analysis, Investigation, Methodology; **Luigia Cristino:** Investigation, Methodology; **Julián Romero:** Funding acquisition, Resources; **Cecilia J. Hillard:** Investigation, Resources; **Rafael Maldonado:** Funding acquisition, Supervision, Resources; **Vincenzo Di Marzo:** Conceptualization, Resources, Writing – review & editing; **Fernando Berrendero:** Conceptualization, Data curation, Formal analysis, Funding acquisition, Investigation, Methodology, Project administration, Resources, Supervision, Writing – original draft, Writing – review & editing.

Declaration of Competing Interest

The authors declare no competing financial interests or personal relationships with other people or organizations that could inappropriately influence their work in this paper.

Data Availability

All data generated or analysed during this study are available from the corresponding author on reasonable request.

Acknowledgements

This work was supported by MICINN [PID2020-116579RB-100/AEI/10.13039/501100011033] and "Ministerio de Economía y Competitividad" MINECO/FEDER, UE [SAF2017-85299-R] to FB and [PID2019-108992-RB-100] to JR, "Plan Nacional sobre Drogas" [#2019I024] to FB and "Proyectos de investigación Universidad Francisco de Vitoria [2018-2019]" to FB. M.T-B and C.I-L are supported by a predoctoral fellowship from Universidad Francisco de Vitoria. Any of the funding sources were involved in the study design and preparation. We are grateful to Dr Rosa María Tolón for her guidance on RT-PCR analyses, and Dr M. Ruth Pazos and Mario Amores for their assistance with microscopy evaluation.

Appendix A. Supporting information

Supplementary data associated with this article can be found in the online version at [doi:10.1016/j.biopha.2022.112925](https://doi.org/10.1016/j.biopha.2022.112925).

References

- [1] L. de Lecea, T.S. Kilduff, C. Peyron, X. Gao, P.E. Foye, P.E. Danielson, et al., The hypocretins: hypothalamus-specific peptides with neuroexcitatory activity, *Proc. Natl. Acad. Sci. USA* 95 (1998) 322–327.
- [2] T. Sakurai, A. Amemiya, M. Ishii, I. Matsuzaki, R.M. Chemelli, H. Tanaka, et al., Orexins and orexin receptors: a family of hypothalamic neuropeptides and G protein-coupled receptors that regulate feeding behavior, *Cell* 92 (1998) 573–585.
- [3] T. Sakurai, The role of orexin in motivated behaviours, *Nat. Rev. Neurosci.* 15 (2014) 719–731.
- [4] Á. Flores, R. Saravia, R. Maldonado, F. Berrendero, Orexins and fear: implications for the treatment of anxiety disorders, *Trends Neurosci.* 38 (2015) 550–559.
- [5] S.B. Li, L. de Lecea, The hypocretin (orexin) system: from a neural circuitry perspective, *Neuropharmacology* 167 (2020), 107993.
- [6] S. Soya, H. Shoji, E. Hasegawa, M. Hondo, T. Miyakawa, M. Yanagisawa, et al., Orexin receptor-1 in the locus coeruleus plays an important role in cue-dependent fear memory consolidation, *J. Neurosci.* 33 (2013) 14549–14557.
- [7] R.M. Sears, A.E. Fink, M.B. Wigstrand, C.R. Farb, L. de Lecea, J.E. Ledoux, Orexin/hypocretin system modulates amygdala-dependent threat learning through the locus coeruleus, *Proc. Natl. Acad. Sci. USA* 110 (2013) 20260–20265.
- [8] Á. Flores, V. Valls-Comamala, G. Costa, R. Saravia, R. Maldonado, F. Berrendero, The hypocretin/orexin system mediates the extinction of fear memories, *Neuropsychopharmacology* 39 (2014) 2732–2741.
- [9] H. Wang, S. Li, G.J. Kirouac, Role of the orexin (hypocretin) system in contextual fear conditioning in rats, *Behav. Brain Res* 316 (2017) 47–53.
- [10] Á. Flores, C. Herry, R. Maldonado, F. Berrendero, Facilitation of contextual fear extinction by orexin-1 receptor antagonism is associated with the activation of

- specific amygdala cell subpopulations, *Int J. Neuropsychopharmacol.* 20 (2017) 654–659.
- [11] S. Salehabadi, K. Abrari, M. Elahdadi Salmani, M. Nasiri, T. Lashkarbolouki, Investigating the role of the amygdala orexin receptor 1 in memory acquisition and extinction in a rat model of PTSD, *Behav. Brain Res* 384 (2020), 112455.
- [12] A.C. Sharko, J.R. Fadel, K.F. Kaigler, M.A. Wilson, Activation of orexin/hypocretin neurons is associated with individual differences in cued fear extinction, *Physiol. Behav.* 178 (2017) 93–102.
- [13] M.H. Monfils, H.J. Lee, N.E. Keller, R.F. Roquet, S. Quevedo, L. Agee, et al., Predicting extinction phenotype to optimize fear reduction, *Psychopharmacol. (Berl.)* 236 (2019) 99–110.
- [14] C. Peyron, J. Faraco, W. Rogers, B. Ripley, S. Overeem, Y. Charnay, et al., A mutation in a case of early onset narcolepsy and a generalized absence of hypocretin peptides in human narcoleptic brains, *Nat. Med* 6 (2000) 991–997.
- [15] A. Ponz, R. Khatami, R. Poryazova, E. Werth, P. Boesiger, S. Schwartz, et al., Reduced amygdala activity during aversive conditioning in human narcolepsy, *Ann. Neurol.* 67 (2010) 394–398.
- [16] P.L. Johnson, W. Truitt, S.D. Fitz, P.E. Minick, A. Dietrich, S. Sanghani, et al., A key role for orexin in panic anxiety, *Nat. Med* 16 (2010) 111–115.
- [17] J.R. Strawn, G.J. Pyne-Geithman, N.N. Ekhtor, P.S. Horn, T.W. Uhde, L.A. Shutter, et al., Low cerebrospinal fluid and plasma orexin-A (hypocretin-1) concentrations in combat-related posttraumatic stress disorder, *Psychoneuroendocrinology* 35 (2010) 1001–1007.
- [18] G. Li, K. Zhang, L. Wang, C. Cao, R. Fang, P.L. Liu, et al., The preliminary investigation of orexigenic hormone gene polymorphisms on posttraumatic stress disorder symptoms, *Psychoneuroendocrinology* 100 (2019) 131–136.
- [19] R. Mechoulam, L.A. Parker, The endocannabinoid system and the brain, *Annu Rev. Psychol.* 64 (2013) 21–47.
- [20] B. Lutz, G. Marsicano, R. Maldonado, C.J. Hillard, The endocannabinoid system in guarding against fear, anxiety and stress, *Nat. Rev. Neurosci.* 16 (2015) 705–718.
- [21] G. Marsicano, C.T. Wotjak, S.C. Azad, T. Bisogno, G. Rammes, M.G. Cascio, et al., The endogenous cannabinoid system controls extinction of aversive memories, *Nature* 418 (2002) 530–534.
- [22] O. Gunduz-Cinar, K.P. MacPherson, R. Cinar, J. Gamble-George, K. Sugden, B. Williams, et al., Convergent translational evidence of a role for anandamide in amygdala-mediated fear extinction, threat processing and stress-reactivity, *Mol. Psychiatry* 18 (2013) 813–823.
- [23] N.D. Hartley, O. Gunduz-Cinar, L. Halladay, O. Bukalo, A. Holmes, S. Patel, et al., 2-arachidonoylglycerol signaling impairs short-term fear extinction, *Transl. Psychiatry* 6 (3) (2016), e749.
- [24] M. Morena, A.S. Nastase, A. Santori, B.F. Cravatt, R.M. Shansky, M.N. Hill, Sex-dependent effects of endocannabinoid modulation of conditioned fear extinction in rats, *Br. J. Pharm.* 178 (2021) 983–996.
- [25] Á. Flores, R. Maldonado, F. Berrendero, Cannabinoid-hypocretin cross-talk in the central nervous system: what we know so far, *Front Neurosci.* 7 (2013) 256.
- [26] F. Berrendero, Á. Flores, P. Robledo, When orexins meet cannabinoids: bidirectional functional interactions, *Biochem Pharm.* 57 (2018) 43–50.
- [27] A. López, N. Aparicio, M.R. Pazos, M.T. Grande, M.A. Barreda-Manso, I. Benito-Cuesta, et al., Cannabinoid CB(2) receptors in the mouse brain: relevance for Alzheimer's disease, *J. Neuroinflamm.* 5 (1) (2018) 158.
- [28] L. Sun, R. Dong, X. Xu, X. Yang, M. Peng, Activation of cannabinoid receptor type 2 attenuates surgery-induced cognitive impairment in mice through anti-inflammatory activity, *J. Neuroinflamm.* 14 (1) (2017) 138.
- [29] G. Paxinos, K.B.J. Franklin, *The Mouse Brain in Stereotaxic Coordinates*, Academic Press, San Diego, CA, USA, 2001.
- [30] L. Palomba, A. Motta, R. Imperatore, F. Piscitelli, R. Capasso, F. Mastroiacovo, et al., Role of 2-arachidonoyl-glycerol and CB1 receptors in orexin-A-mediated prevention of oxygen-glucose deprivation-induced neuronal injury, *Cells* 9 (6) (2020) 1507.
- [31] R.A. Rice, J. Pham, R.J. Lee, A.R. Najafi, B.L. West, K.N. Green, Microglial repopulation resolves inflammation and promotes brain recovery after injury, *Glia* 65 (2017) 931–944.
- [32] V. Di Marzo, L. De Petrocellis, T. Bisogno, The biosynthesis, fate and pharmacological properties of endocannabinoids, *Handb. Exp. Pharm.* 168 (2005) 147–185.
- [33] S. Maren, K.L. Phan, I. Liberzon, The contextual brain: implications for fear conditioning, extinction and psychopathology, *Nat. Rev. Neurosci.* 14 (2013) 417–428.
- [34] R.A. Kohman, J.S. Rhodes, Neurogenesis, inflammation and behavior, *Brain Behav. Immun.* 27 (2013) 22–32.
- [35] S. Zou, U. Kumar, Cannabinoid receptors and the endocannabinoid system: signaling and function in the central nervous system, *Int J. Mol. Sci.* 19 (3) (2018) 833.
- [36] A. Adeluyi, L. Guerin, M.L. Fisher, A. Galloway, R.D. Cole, S.S.L. Chan, et al., Microglia morphology and proinflammatory signaling in the nucleus accumbens during nicotine withdrawal, *Sci. Adv.* 5 (10) (2019) eaax7031.
- [37] G. Salvatore, P. Bonaventure, A. Shekhar, P.L. Johnson, B. Lord, B.T. Shireman, et al., Translational evaluation of novel selective orexin-1 receptor antagonist JNJ-61393215 in an experimental model for panic in rodents and humans, *Transl. Psychiatry* 10 (1) (2020) 308.
- [38] Y.C. Ho, H.J. Lee, L.W. Tung, Y.Y. Liao, S.Y. Fu, S.F. Teng, et al., Activation of orexin 1 receptors in the periaqueductal gray of male rats leads to antinociception via retrograde endocannabinoid (2-arachidonoylglycerol)-induced disinhibition, *J. Neurosci.* 31 (2011) 14600–14610.
- [39] H.J. Lee, L.Y. Chang, Y.C. Ho, S.F. Teng, L.L. Hwang, K. Mackie, et al., Stress induces analgesia via orexin 1 receptor-initiated endocannabinoid/CB1 signaling in the mouse periaqueductal gray, *Neuropharmacology* 105 (2016) 577–586.
- [40] Y.H. Chen, H.J. Lee, M.T. Lee, Y.T. Wu, Y.H. Lee, L.L. Hwang, et al., Median nerve stimulation induces analgesia via orexin-initiated endocannabinoid disinhibition in the periaqueductal gray, *Proc. Natl. Acad. Sci. USA* 115 (2018) E10720–E10729.
- [41] G. Morello, R. Imperatore, L. Palomba, C. Finelli, G. Labruna, F. Pasanisi, et al., Orexin-A represses satiety-inducing POMC neurons and contributes to obesity via stimulation of endocannabinoid signaling, *Proc. Natl. Acad. Sci. USA* 113 (2016) 4759–4764.
- [42] N. Forte, S. Boccella, L. Tunisi, A.C. Fernández-Rilo, R. Imperatore, F.A. Iannotti, et al., Orexin-A and endocannabinoids are involved in obesity-associated alteration of hippocampal neurogenesis, plasticity, and episodic memory in mice, *Nat. Commun.* 12 (1) (2021) 6137.
- [43] L.W. Tung, G.L. Lu, Y.H. Lee, L. Yu, H.J. Lee, E. Leishman, et al., Orexins contribute to restraint stress-induced cocaine relapse by endocannabinoid-mediated disinhibition of dopaminergic neurons, *Nat. Commun.* 7 (2016) 12199.
- [44] T. Bisogno, A. Mahadevan, R. Coccorello, J.W. Chang, M. Allarà, Y. Chen, et al., A novel fluorophosphate inhibitor of the biosynthesis of the endocannabinoid 2-arachidonoylglycerol with potential anti-obesity effects, *Br. J. Pharm.* 169 (2013) 784–793.
- [45] R.N. Ruggiero, M.T. Rossignoli, D.B. Marques, B.M. de Sousa, R.N. Romcy-Pereira, C. Lopes-Aguiar, et al., Neuromodulation of hippocampal-prefrontal cortical synaptic plasticity and functional connectivity: implications for neuropsychiatric disorders, *Front Cell Neurosci.* 15 (2021), 732360.
- [46] I. Katona, T.F. Freund, Multiple functions of endocannabinoid signaling in the brain, *Annu Rev. Neurosci.* 35 (2012) 529–558.
- [47] I. Jenniches, S. Ternes, O. Albayram, D.M. Otte, K. Bach, L. Bindila, et al., Anxiety, stress, and fear response in mice with reduced endocannabinoid levels, *Biol. Psychiatry* 79 (2015) 858–868.
- [48] C. Chu, M.H. Murdock, D. Jing, T.H. Won, H. Chung, A.M. Kressel, et al., The microbiota regulate neuronal function and fear extinction learning, *Nature* 574 (2019) 543–548.
- [49] C. Manca, M. Shen, B. Boubertakh, C. Martin, N. Flamand, C. Silvestri, et al., Alterations of brain endocannabinoid signaling in germ-free mice, *Biochim Biophys. Acta Mol. Cell Biol. Lipids* 1865 (12) (2020), 158786.
- [50] C. Sánchez, M.L. de Ceballos, T. Gomez del Pulgar, D. Rueda, C. Corbacho, G. Velasco, et al., Inhibition of glioma growth in vivo by selective activation of the CB(2) cannabinoid receptor, *Cancer Res* 61 (2001) 5784–5789.
- [51] C. Benito, E. Núñez, R.M. Tolón, E.J. Carrier, A. Rábano, C.J. Hillard, et al., Cannabinoid CB2 receptors and fatty acid amide hydrolase are selectively overexpressed in neuritic plaque-associated glia in Alzheimer's disease brains, *J. Neurosci.* 23 (2003) 11136–11141.
- [52] J.M. Robertson, J.K. Achua, J.P. Smith, M.A. Prince, C.D. Staton, P.J. Ronan, et al., Anxious behavior induces elevated hippocampal CB2 receptor gene expression, *Neuroscience* 352 (2017) 273–284.
- [53] D. Ivy, F. Palese, V. Vozella, Y. Fotio, A. Yalcin, G. Ramirez, et al., Cannabinoid CB2 receptors mediate the anxiolytic-like effects of monoacylglycerol lipase inhibition in a rat model of predator-induced fear, *Neuropsychopharmacology* 45 (2020) 1330–1338.
- [54] I. Banaszkiewicz, G. Biala, M. Kruk-Slomka, Contribution of CB2 receptors in schizophrenia-related symptoms in various animal models: Short review, *Neurosci. Biobehav. Rev.* 114 (2020) 158–171.
- [55] G. Bedse, M.N. Hill, S. Patel, 2-Arachidonoylglycerol modulation of anxiety and stress adaptation: from grass roots to novel therapeutics, *Biol. Psychiatry* 88 (2020) 520–530.
- [56] M.S. García-Gutiérrez, A. Ortega-Álvarez, A. Busquets-García, J.M. Pérez-Ortiz, L. Caltana, M.J. Ricatti, et al., Synaptic plasticity alterations associated with memory impairment induced by deletion of CB2 cannabinoid receptors, *Neuropharmacology* 73 (2013) 388–396.
- [57] A.M. Raymundi, T.R. da Silva, J.M.B. Sohn, L.J. Bertoglio, C.A. Stern, Effects of Δ9-tetrahydrocannabinol on aversive memories and anxiety: a review from human studies, *BMC Psychiatry* 20 (1) (2020) 420.
- [58] M.O. Bonn-Miller, S. Sisley, P. Riggs, B. Yazarr-Klosinski, J.B. Wang, M.J.E. Loflin, et al., The short-term impact of 3 smoked cannabis preparations versus placebo on PTSD symptoms: a randomized cross-over clinical trial, *PLoS One* 16 (3) (2021), e0246990.
- [59] J.A. Komorowska-Müller, A.C. Schmöle, CB2 receptor in microglia: the guardian of self-control, *Int J. Mol. Sci.* 22 (1) (2020) 19.
- [60] J.A. Sumner, K.M. Nishimi, K.C. Koenen, A.L. Roberts, L.D. Kubzansky, Posttraumatic stress disorder and inflammation: untangling issues of bidirectionality, *Biol. Psychiatry* 87 (2020) 885–897.
- [61] Z. Yu, H. Fukushima, C. Ono, M. Sakai, Y. Kasahara, Y. Kikuchi, et al., Microglial production of TNF-alpha is a key element of sustained fear memory, *Brain Behav. Immun.* 59 (2017) 313–321.
- [62] I.C. Passos, M.P. Vasconcelos-Moreno, L.G. Costa, M. Kunz, E. Brietzke, J. Quevedo, et al., Inflammatory markers in post-traumatic stress disorder: a systematic review, meta-analysis, and meta-regression, *Lancet Psychiatry* 2 (2015) 1002–1012.